HHS Public Access

Author manuscript

Osteoarthritis Cartilage. Author manuscript; available in PMC 2021 July 01.

Published in final edited form as:

Osteoarthritis Cartilage. 2020 July ; 28(7): 966–976. doi:10.1016/j.joca.2020.04.004.

Suppression of Circadian Clock Protein Cryptochrome 2 Promotes Osteoarthritis

Hirofumi Bekki[*], **Tomas Duffy**[*], **Naoki Okubo**, **Merissa Olmer**, **Oscar Alvarez-Garcia**, **Katja Lamia**, **Steve Kay**, **Martin Lotz**

Department of Molecular Medicine, Scripps Research, La Jolla, CA

Abstract

OBJECTIVES: Abnormal chondrocyte gene expression promotes osteoarthritis (OA) pathogenesis. A previous RNA-sequencing study revealed that circadian rhythm pathway and expression of core clock gene cryptochrome 2 (*CRY2*) are dysregulated in human OA cartilage. Here we determined expression patterns and function *CRY1* and *CRY2*.

METHODS: CRY mRNA and protein expression was analyzed in normal and OA human and mouse cartilage. Mice with deletion of *Cry1* or *Cry2* were analyzed for severity of experimental OA and to determine genes and pathways that are regulated by *Cry*.

RESULTS: In human OA cartilage, CRY2 but not CRY1 staining and mRNA expression was significantly decreased. Cry2 was also suppressed in mice with aging-related OA. *Cry2* KO but not *Cry1* KO mice with experimental OA showed significantly increased severity of histopathological changes in cartilage, subchondral bone and synovium. In OA chondrocytes, the levels of *CRY1* and *CRY2* and the amplitude of circadian fluctuation were significantly lower. RNA-seq on knee articular cartilage of wild-type and *Cry2* KO mice identified 53 differentially expressed genes, including known *Cry2* target circadian genes *Nr1d1*, *Nr1d2*, *Dbp* and *Tef*. Pathway analysis that circadian rhythm and extracellular matrix remodeling were dysregulated in *Cry2* KO mice.

CONCLUSIONS: These results show an active role of the circadian clock in general, and of *CRY2* in particular, in maintaining ECM homeostasis in cartilage. This cell autonomous network of circadian rhythm genes is disrupted in OA chondrocytes. Targeting *CRY2* has potential to correct abnormal gene expression patterns and reduce the severity of OA.

Corresponding Author: Martin Lotz, mlotz@scripps.edu, Tel 858 785 8960.

[*]Authors contributed equally

AUTHOR CONTRIBUTIONS

ML, SK, KL, HO, HB and TD made substantial contributions to the conception and design of the study. HO, HB, TD and MO performed experiments and analyzed data.

All authors contributed to the interpretation of results. ML wrote the first draft. All authors contributed to the final version of the manuscript. HB, TD and ML have full access to the data and take responsibility for the content and guarantees the integrity and accuracy of the work undertaken. All authors have read, provided critical feedback on intellectual content and approved the final manuscript.

CONFLICT OF INTEREST

The authors have no conflict of interest.

INTRODUCTION

Recent advances in OA research led to the identification of signaling mechanisms and pathways that are abnormally activated in OA and contribute to cartilage damage[1,2]. We completed an RNA-seq study on normal and OA human knee cartilage that led to the discovery that the circadian rhythm (CR) pathway was inhibited and the most significantly dysregulated pathway in OA[3]. CR is critical in coordinating cell functions throughout all tissues including sleep/wake cycles, blood pressure, body temperature and metabolism[4,5]. CR is regulated by the central oscillator in the hypothalamic suprachiasmatic nucleus (SCN). Cell autonomous local oscillators throughout the body coordinate daily cycles by integrating signals from the SCN with other internal and external time cues. The pacemaker consists of a core group of genes with transcriptional-translational feedback loops that involve multiple clock genes encoding the transcription factors circadian locomotor output cycles kaput (*CLOCK*), brain and muscle ARNT-like 1 (*BMAL1*), *CRY*, and period[6]. Forming a heterodimer, *CLOCK* and *BMAL1* drive transcription of target genes, including those encoding their own repressors period (*PER1, PER2, PER3*) and *CRY1* and *CRY2*. *PER* and *CRY* dimerize and repress *CLOCK* and *BMAL1*[6,7]. These clock genes and their protein products function in a feedback loop resulting in a nearly 24-hour cycle. The transcription factor *BMAL1* is the core driver of the molecular clock. Positive regulators (*BMAL1, CLOCK, NPAS2*) stimulate the expression of negative feedback regulators (*PER, CRY, NR1D1*), which in turn inhibit the expression and activity of the positive regulators[8].

The circadian clock coordinates tissue function through control of tissue-specific sets of genes. Depending on the tissue and the stringency of the analysis, the core clock directly or indirectly drives oscillating transcription, ranging from 10% to more than 40% of all protein coding genes[9–12]. In articular cartilage, 615 genes, representing 3.9% of total transcripts in cartilage tissue were expressed in a circadian manner[13].

Autonomous clocks have been demonstrated in most peripheral tissues and cultured cells[14,15], including in cartilage and chondrocytes[13,16]. We reported that *NR1D1* and *BMAL1* mRNA and protein levels were significantly reduced in OA compared to normal cartilage[3]. In cultured normal human chondrocytes, a clear circadian rhythmicity was observed for *NR1D1* and *BMAL1*. Sequencing of RNA from chondrocytes treated with *NR1D1* or *BMAL1* siRNA identified 330 and 68 significantly different genes, respectively, and this predominantly affected the TGF-β signaling pathway[3]. BMAL1 expression was reduced in human OA and aging mouse cartilage[17]. Conditional *Bmal1*-deficient mice developed progressive cartilage degeneration in knee but not in hip[17]. *BMAL1* knock down in normal chondrocytes also increased proliferation and *MMP13* expression[18].

Previously, we performed an RNA-seq analysis of normal and OA human articular cartilage and found that *CRY2* is significantly reduced in OA[19]. The objective of the study was to analyze the function of *CRY1/2* in cartilage *in vitro* and *in vivo*. The hypothesis was that *CRY* genes regulate gene expression in chondrocytes and that abnormal gene expression related to *CRY* suppression increases OA severity.

MATERIALS AND METHODS

Human Cartilage Donors

Normal human knee cartilage tissues were procured by tissue banks (approved by Scripps Institutional Review Board) and processed within 24–72 hours post mortem. Knees from healthy donors were selected by tissue banks and cases with a history of joint injury, arthritis or surgery were excluded. The entire knees were obtained and upon opening the joints, the macroscopic appearance of cartilage, menisci, synovium and ligaments was assessed and graded according to the Outerbridge system for cartilage[20] and the Pauli method for menisci[21]. Samples from all joint tissues were also analyzed by histology to confirm the absence of pathological changes. For OA donors, tissues were obtained from patients undergoing knee arthroplasty, representing end-stage OA. The tissue blocks from normal donors were resected from the central weight-bearing area of the medial femoral condyle. In the OA cases, the harvest site was moved more proximal or distal in cases where the entire cartilage had been destroyed. Full thickness cartilage was harvested for RNA isolation from identical locations on the medial femoral condyles. Differernt cartilage samples were used for IHC, cell and RNA isolation.

Primary articular chondrocyte preparation and culture

Chondrocytes were isolated from both OA and normal cartilage using the same protocol. Approximate $5cm^3$ of cartilage slices were collected from femoral condyles and transferred into 2mg/ml collagenase IV (Worthington Biochemical, Lakewood, NJ) diluted in DMEM and incubated on a shaker at 37° degrees for 24 h with rotation at 1500 rpm, Cells were plated into dishes and after having reached 70–80% confluence, the cells were trypsinized and used in experiments.

Circadian Rhythmicity in Cultured Chondrocytes

We used chondrocytes from 4 normal and 5 OA donors. Cultured chondrocytes were maintained in DMEM with 10% calf serum supplemented with penicillin and streptomycin. Medium was changed to 0.5% serum with 100nM dexamethasone one hour before medium change to serum-free-DMEM. T0 was defined as 24 hours after medium change to serum-free-DMEM. Cells were collected every four hours for the time course analysis of gene expression. RNA was isolated and RT-qPCR performed as described[25].

Immunohistochemistry

Normal and OA cartilage were from nine donors (4 male and 5 female, median 34 years) and 10 donors (3 male and 7 female, median 69 years), respectively.

Immunohistochemistry was performed to assess protein expression patterns in human and mouse cartilage using anti-CRY1-CT and anti-CRY2-CT as described[22].

As as primary antibodies we used polyclonal antibodies raised in guinea pigs against the C-termini of *Cry1* (amino acids 583–606) or *Cry2* (amino acids 563–592). Stock concentration was 0.65mg/mL and they were diluted at 1:100. Rabbit IgG (1 μg/ml) was used as a negative control in all experiments. For human cartilage, expression patterns were compared between

normal and OA samples. In C57 BL/6 mice, we analyzed young normal and aged knees as a model of aging-related OA. We also analyzed knees from mice with surgically induced OA by destabilization of medial meniscus and medial collateral ligament resection[23]. The methods for tissue processing and immunohistochemistry were described earlier[23]. Cells positive for CRY1/2 were counted in one osteochondral section per donor and five fields per section. The area examined was the cartilage tissue above the tidemark in the tibial cartilage and determined as the ratio of the total number of positive cells to the total number of chondrocytes in the section. Two individual researchers blinded to the group allocations evaluated histological sections.

Cartilage RNA Isolation

We isolated RNA from human cartilage from 6 female (age 33–58 years, mean 48.7 years) and 6 male (age 18–56 years, mean 40.3 years) donors for PCR analysis. Cartilage was stored at −20°C in Allprotect Tissue Reagent (Qiagen, Valencia, CA) immediately after resection from the subchondral bone. RNA was extracted from human cartilage as described[25]. In brief, cartilage was pulverized in a 6770 Freezer/Mill Cryogenic Grinder (SPEX SamplePrep, Metuchen, NJ), and homogenized in Qiazol Lysis Reagent (Qiagen) using 25mg tissue per 700ul Qiazol. RNA was isolated using the miRNeasy Mini kit (Qiagen) with on-column DNAse digestion, followed by removal of proteoglycans using RNAmate (BioChain Institute, Newark, CA).

Mouse articular cartilage was collected from both sides of the femoral condyle and tibial plateau from 3-month-old mice.

For mouse cartilage, since the amount of cartilage and RNA from it is small, we added chloroform to purify the RNA. After TRIzol solubilization, the addition of chloroform causes phase separation, where protein is extracted to the organic phase, DNA resolves at the interface, and RNA remains in the aqueous phase. We collected only the RNA layer and RNA was isolated following the protocol for the miRNeasy Mini kit (Qiagen)[24].

Quantitative Polymerase Chain Reaction (qPCR)

Real-time PCR was performed on a Light Cycler 480 instrument (Roche Diagnostics) using TaqMan probes The following pre-designed TaqMan gene expression assays (Life Technologies) were used: *GAPDH* (Hs02758991_g1), *Gapdh* (Mm99999915_g1 *CRY1* (Hs00172734_m1), *CRY2* (Hs00323654_m1), *Dbp* (Mm00497539_m1), Nr1d1 (Mm00520708_m1), *Tek* (Mm00443243_m1), *Col22a* (Mm01195058_m1).

Mice

All animal studies were performed with approval by the Scripps Institutional Animal Care and Use Committee. Mice with global deletion of *Cry1* or *Cry2*[22,26] on C57/BL6 background were obtained from Katja Lamia. $Cry1^{-/-}$ and $Cry2^{-/-}$ mice were generated by Katja Lamia as described[22]. Genotyping was performed by PCR using tail DNA. $Cry^{+/+}$ littermates were used as controls. We used mice from different litters in each of the experiments. Mice from different litters were assigned to each of the experiments at the same ratio.

Experimental OA in Mice

Surgical OA model was created by destabilizing the medial meniscus (DMM) in four months old skeletally mature mice as described[27]. Right knees were DMM surgery side, and we use left knees as controls. Eight weeks after DMM surgery, knee joints were collected for analysis.

Histological Analyses of Mouse Joints

Knee joints were collected from 5-month-old control, *Cry1* and *Cry2* KO mice. The entire knee joints were fixed in 10% zinc buffered formalin for 2 days, decalcified in TBD-2 for 24 h. We used a standardized selection of the sections from the mouse knee joint that were scored in the mouse DMM model. Sections were cut from the periphery of the joint until the central weigh-bearing area of the medial compartment of the knee joints was reached, using meniscus as landmark. This area is where lesions in the DMM model are most severe. Sections were stained with Safranin-O–fast green and picrosirius red staining for further analysis. Histological scoring of OA-like changes on the medial femoral condyle and the medial tibial plateau was performed using the Osteoarthritis Research Society International (OARSI) cartilage OA histopathology semi-quantitative scoring system (score 0–40)[28]. Synovial changes were evaluated using Krenn's synovitis scoring system (score 0–9)[29]. We used a modified bone scoring system (score 0–4) as previously described[30]. We evaluated lamellar structure (>50% replaced: 1), angiogenesis (vessels of Rt side>Lt side: 1), ectopic ossification (≥2 pieces: 1) and periarticular bone change (+: 1) in the tibia.

RNA-sequencing of Mouse Cartilage

Total RNA was extracted from femoral and tibial cartilage of 3 WT and 3 *Cry2* KO mice. The RIN numbers from WT mice were 6.3, 6.3, 5.6. The RIN numbers for *Cry2* KO mice were 4.5, 5.0, 4.7, respectively. The RNA concentration was 50pg/μl. In the SMART-Seq v4 kit rRNA is cleaved after cDNA synthesis. Poly-A selection was not performed. Libraries were prepared using the SMART-Seq v4 Ultra Low Input RNA Kit (Clontech). Approximately, 30 million 75 bp single-end reads per sample were sequenced on a Nextseq500 (Illumina). Briefly, adapters and low quality bases were removed using TrimGalore (https://github.com/FelixKrueger/TrimGalore) and mapped to the mouse mm9 genome using STAR[31]. Raw counts were obtained using featureCounts[32]. Differential gene expression analysis was carried out with DESeq2[33]. Genes with an adjusted p-value <0.05 were considered differentially expressed. Pathway analysis was conducted using the findGO.pl script from the HOMER package[34]. The protein–protein association network was constructed using STRING database[35].

Statistical Analysis

Data sets were evaluated and results were analyzed using JMP version 13 (SAS Institute Inc., NC) and GraphPad Prism version 8.0.0 for Windows, GraphPad Software, San Diego, California USA, www.graphpad.com". Statistical tests were chosen according to the type of experimental design and variables. Specifically, the significance of the difference of medians between pairs of groups was determined by Mann-Whitney test, which was used to determine *CRY* expression patterns in human and mouse cartilage since this non-parametric

test is known to be more statistically powerful when the distribution is not normal. Hodges-Lehmann (HL) estimate which is the median of difference between the two groups, the confidence interval for this estimate and exact p values were reported for Mann-Whitney test results. The non parametric results are reported as median +/− interquartile range (IQR).

For categorical measures (angiogenesis), Fisher's Exact test was used. The expression data that was collected over 13 time points was analyzed using repeated measures ANOVA that is based on GLM. The normality and homoscedasticity assumptions were checked with Shapiro-Wilk W test and with residual vs. predicted plots respectively. Mouse body weight and length per treatment groups were compared using Welch's ANOVA test unequal variances. For the multiple comparison, the statistical analysis was conducted by Steel test to determine the difference in body size and histological scores between WT mice and mutant mice. Confidence intervals (CI) was also calculated for multiple comparisons. Values less than 0.05 were considered significant.

RESULTS

Suppression of CRY mRNA and protein in aging and OA-affected cartilage in human and mouse joints

We performed PCR analysis to confirm our prior findings from RNA-seq analysis of normal and OA human cartilage which showed that circadian rhythm was a significantly dysregulated pathway and that *CRY2* was among the repressed genes[3,19]. PCR analysis of additional human cartilage confirmed reduced *CRY2* (P=0.0007) but not *CRY1* expression in OA (P=0.89) (Figure 1A). For *CRY1*, the median relative expression levels of *GAPDH* was 0.93 (0.68–1.32) in normal cartilage and 0.90 (0.74–1.2) in OA cartilage, with Hodges-Lehman difference of 0.015 (CI 95.51%=−0.36 to 0.26). For *CRY2*, the relative expression levels of *GAPDH* was 0.96 (0.59–1.38) in normal cartilage and 0.48 (0.33–0.64) in OA cartilage (Figure 1A) with Hodges-Lehman difference of −0.49 (CI 95.51%=−0.82 to −0.18).

Immunohistochemical analysis showed that in normal human articular cartilage CRY1 and CRY2 proteins are expressed throughout all zones, most strongly in the superficial and mid zones. In OA cartilage, CRY2 positive cells were diminished even in areas of preserved full thickness cartilage, with few positive cells remaining in the superficial zone. In lesions with fibrillations, strong staining was observed in chondrocyte clusters (Figure 1B). For CRY2, the median positive cell ratio was 0.45 (0.32–0.51) in normal cartilage and 0.24 (0.18–0.32) in OA cartilage, and there was a significant difference between these two ratios (Hodges-Lehman difference of −0.16, CI 95.7%=−0.27 to −0.05, P=0.013). There was a trend towards reduced CRY1 positive cells in OA, but this was not significant. The median positive cell ratio was 0.37 (0.25–0.45) in normal cartilage and 0.26 (0.15–0.33) in OA cartilage (Hodges-Lehman difference of −0.11, CI 95.7%=−0.21 to 0.009, P=0.07).

In normal mature mouse knee joints Cry protein expression was detected in all zones of articular cartilage (Figure 2). Cry2 positive cells in knee cartilage were significantly lower in 24 months old mice compared to 6 months old mice (Hodges-Lehman difference of −0.36 (CI 96.97%=−0.64 to −0.13, P=0.03). The positive cell ratio was 0.61 (0.46–0.74) in

cartilage from 6 months old mice and 0.34(0.05–0.36) in cartilage from 24 months old mice. Although not significant, there was a trend towards reduced Cry1 positive cells at 24 months. The positive cell ratio was 0.53 (0.38–0.63) at 6 months and 0.34(0.03–0.51) at 24 months (Hodges-Lehman difference of −0.19 (CI 96.83%=−0.58 to 0.10, P=0.09) (Figure 2).

Dysregulated *CRY* expression and abnormal rhythm in cultured human OA chondrocytes

To further analyze OA-associated differences in CRY and circadian rhythm, we compared cultured human chondrocytes from normal and OA knee joints. In normal chondrocytes levels of *CRY1* mRNA expression peaked at T8 and T36, with lowest expression observed at T20. Repeated measures ANOVA was applied to interrogate the effect of time, OA treatment and their interaction on CRY1 mRNA expression, OA and normal chondrocytes had different levels of CRY1 expression over the 13 timepoints (Time × Treatment, $F_{12,84}$=7.28, P<0.0001), overall normal and OA treatments resulted in different expression levels (Treatment, $F_{1,7}$=8.49, P=0.0225), where OA chondrocytes had higher expression (mean difference 0.38, CI %95= −0.7 to −0.07) and overall the expression levels varied over the 13 time points (Time, $F_{12,84}$=24.59, P<0.0001). *CRY2* mRNA expression peaked at T24, with lowest expression at T12. Repeated measures ANOVA was applied to interrogate the effect of time, OA treatment and their interaction on CRY2 mRNA expression, OA and normal chondrocytes had different levels of CRY2 expression over the 13 timepoints (Time × Treatment, $F_{12,84}$=3.15, P=0.001), overall normal and OA treatments resulted in different expression levels (Treatment, $F_{1,7}$=13.54, P=0.008) where OA chondrocytes had higher expression (mean difference −0.24, CI %95= −0.4 to −0.09). Finally, overall the expression levels varied over the time points (Time, $F_{12,84}$=21.34, P<0.0001) (Figure 3).

Skeletal phenotype of *Cry* deficient mice

To assess *CRY* function in cartilage, we used mice with deletion of *Cry1* or *Cry2*. *Cry2* KO and *Cry1* KO mice had normal body weight and length at 1 and 5 months and none of the treatment groups differed per time point for weight (1 month $W_{(2,10.53)}$=1.61, P=0.25, 5 month $W_{(2,11)}$=2.1, P=0.16) or length (1 month $W_{(2,9.3)}$=2.5, P=0.13, 5 month $W_{(2,9.8)}$=1.4, P=0.28) (Figure 4A,B). On histological analysis of the knee joints, the articular cartilage of 5 months old mice did not show any structural defects in the Cry mutant strains (Figure 4B).

The median whole articular cartilage thickness was 100.6 (96.6–103.9) in WT, 103.6 (99.8–107.3) in *Cry1* KO and 108.9 (103.5–111) in *Cry2* KO mice. Whole articular cartilage thickness was not different across Wt and CRY1 (Hodges-Lehman difference of −2.7 (CI 96.50%=−8.8 to 3, P=0.42), however it was higher in CRY2 compared to WT (Hodges-Lehman difference of −7.5 (CI 96.50%=−13 to −0.7, P=0.035).The median height of non-calcified zone was 52.7 (48.4–60.6) in WT, 60.5 (57.3–66.3) in *Cry1* KO and 64.8 (60.6–66.5) in *Cry2* KO mice. The median height of calcified zone was 46.2 (42.5–50.4) in WT, 42.3 (40.5–44.6) in *Cry1* KO and 48 (43.1–52.8) in *Cry2* KO mice. The height of the non-calcified zone was significantly larger in the *Cry2* KO compared to WT mice (Hodges-Lehman difference of −9.6 (CI 96.50%=−17 to −2.5, P=0.008). (Figure 4B). *Cry1* KO mice had increased thickness of the non-calcified zone similar to *Cry2* KO mice, but no there was no significant difference (Hodges-Lehman difference of −6.7 (CI 96.50%=−15 to 1.2, P=0.07) (Figure 4B).

Increased OA severity in *Cry* deficient mice

To determine whether *CRY* protects against cartilage damage, we subjected WT and *Cry* mutant mice to DMM to induce OA. The number of mice were 12 (6 male, 6 female 6) in WT, 13 (7 male, 6 female) in *Cry1* KO, 12 (7 male, 5 female) in *Cry2* KO, respectively. Median OARSI scores were 8.5 (7.3–11.5) in WT, 12 (0–15.5) in *Cry1* KO and 15 (10.8–24.8) in *Cry2* KO mice. Bone scores were 1 (0–2) in WT, 1 (1–2.5) in *Cry1* KO and 2 (2–3.5) in *Cry2* KO mice. Synovium scores were 1.5 (1–2) in WT, 2 (1–2.5) in *Cry1* KO and 3 (2–3) in *Cry2* KO mice. These results showed that experimental OA, as assessed by OARSI scoring, was significantly more severe in the *Cry2* KO mice compared to WT (Hodges-Lehman difference of −6 (CI 96.50%= −12 to −1, P=0.006) but not in *Cry1* KO mice (Hodges-Lehman difference of −4 (CI 95.43%= −7 to 0, P=0.07) (Figure 5). Control left knees did not show differences among the three genotypes (data not shown). The changes in synovium (Hodges-Lehman difference of −1 (CI 95.51%= −2 to 0, P=0.006) and in subchondral bone (Hodges-Lehman difference of −1 (CI 95.50%= −2 to 0, P=0.006) which included increased numbers of blood vessels were also significantly more severe in the *Cry2* KO mice (Figure 5). For angiogenesis, 10 out of 12 *Cry2* KO (83%) and 4 out of 12 WT (33%) mice showed more capillary vessels compared to control knees, respectively. The ratio of *Cry2* KO mice was significantly higher than that of WT mice (Fisher's exact test, P=0.036.

Dysregulated circadian rhythm and extracellular matrix homeostasis in Cry2 KO mice

In order to identify candidate genes and pathways responsible for the increased OA severity in *Cry2* KO mice, we performed RNA-seq on knee articular cartilage of WT and *Cry2* KO mice. Importantly, samples were collected at the time point when *Cry2* levels peak in WT mice, and thus when largest changes are expected. Nevertheless, since *CRY2* functions are partially redundant with *CRY1* and *Cry2* KO alone does not abolish the circadian clock[36], a subtle phenotype is expected. We identified 53 differentially expressed genes (DEG), which includes 4 known *Cry2* target circadian genes *Nr1d1*, *Nr1d2*, *Dbp* and *Tef* (Figure 6).

To identify a putative mechanism by which *Cry2* KO increases the severity of OA, we identified pathways over-represented among the DEG. Interestingly, the top 2 non-redundant over-represented pathways in Reactome DB associated with ECM and the circadian clock. We also performed the analysis using the GO Biological Process DB and the top 2 non-redundant over-represented pathways are angiogenesis and rhythmic process (Figure 6). To better understand the relationship between these pathways we performed a protein-protein interaction network with STRING-DB. We observed that genes belonging to the same pathway are highly interconnected with each other. Particularly interesting is *Pdgfra* since it belongs to both the angiogenesis and CR pathways while having connections to several important genes of the ECM pathway. These results suggest an active role of the circadian clock in general, and of *Cry2* in particular, in maintaining homeostasis of articular cartilage.

To validate the differences in RNA-seq between WT and *Cry2* KO mice, we performed RT-qPCR for *Dbp*, *Nr1d1*, *Tek* and *Col22a* using additional 9 WT and 9 *Cry2* KO mice. For *Dbp*, the median relative expression levels to *Gapdh* was 0.86 (0.68–1.21) in WT cartilage and 9.31 (6.17–10.96) in *Cry2*-KO cartilage (Hodges-Lehman difference of −8.4 (CI

96.00%= −10 to −5.2, P=<0.0001). For *Nr1d1*, the median relative expression levels to *Gapdh* was in 0.55 (0.14–1.36) in WT cartilage and 4.58 (3.4–6.38) in *Cry2*-KO cartilage (Hodges-Lehman difference of −4.4 (CI 95.82%= −6.2 to −1.9, P=0.0007). For *Tek*, the relative expression levels to *Gapdh* was in 0.87 (0.49–1.67) in WT cartilage and 2.3 (1.36–5.13) in *Cry2*-KO cartilage (Hodges-Lehman difference of −1.4 (CI 96.00%= −4.2 to −0.5 P=0.0056). For *Col22a*, the relative expression levels to *Gapdh* was in 1.11 (0.36–1.44) in WT cartilage and 1.76 (1.29–2.51) in *Cry2*-KO cartilage (Hodges-Lehman difference of −0.83 (CI 96.00%= −1.5 to −0.16, P=0.02). *Cry2*-KO mice showed significantly upregulated expression levels for all four genes (Suppl. Fig. 1).

DISCUSSION

Recent studies addressed the function of several CR factors, including NR1D1, *BMAL1*[3,17,37] and *Clock* or *Csnk1*[38] in cartilage and OA. Our present study focused on *CRY2* as our prior RNA-seq study showed that *CRY2* was significantly reduced in human OA[19]. The current results confirm and extend these observations and show that in normal mouse and human cartilage CRY2 is expressed in all zones of articular cartilage. CRY2 protein expression is reduced in human OA cartilage and mouse OA cartilage. The suppression of *CRY2* is also seen in cultured human OA chondrocytes which have reduced amplitudes of *CRY2* fluctuation. Previous showed that autonomous cartilage circadian rhythms in mice became dysregulated with age and upon chronic inflammation[16,39–41]. The studies in mice suggest an age related change in *Cry* expression. The human normal and OA samples were not age matched, with the OA donors being older and it is thus not possible to determine whether the CRY expression changes in human cartilage were primary age or OA-related. In addition, the human OA samples were primary female (11:1) and the the changes reported here can not be generalized to males.

To determine whether the suppression of *Cry2* affects cartilage homeostasis or OA severity we analyzed *Cry* KO mice. *Cry2* and *Cry1* KO mice had normal body weight and length, and these mice did not show any spontaneous cartilage degradation by 5 months of age. It is possible that *Cry* deficient mice will manifest earlier onset of aging-related OA at more advanced age and this needs to be determined in future studies. In the DMM model, there was significantly more severe cartilage damage in the *Cry2* KO mice but not in the *Cry1* KO mice. This was observed in male and female mice. These results show that *Cry2* but not *Cry1* has chondroprotective effects in mouse knees subjected to DMM surgery. Associated with more severe cartilage damage were also more severe subchondral bone changes and synovial inflammation in the *Cry2* KO mice.

Although *CRY1* and *CRY2* interact and repress *Clock/Bmal1*[42] and several nuclear receptors (NRs)[43], both CRY proteins have differential and selective roles in defining the pace of the circadian clock and its outputs. *CRY1* is a more potent repressor of *Clock/Bmal1*-mediated transcriptional activation than *CRY2*, leading to stronger circadian phenotypes when each is individually suppressed[44]. On the other hand, many NRs display increased affinity for *CRY2* compared with *CRY1*[43]. Furthermore, integration of mouse liver ChIP-seq data shows *Cry1* as the main interactor of *Clock/Bmal1* on chromatin, while *Cry2* binding is mostly co-occupied by NRs[43,45].

Furthermore, only *CRY2* but not *CRY1* serves as a component of an E3 ligase complex that ubiquitinates c-Myc prior to its degradation[46] and *CRY2* but not *CRY1* promotes myoblast proliferation and subsequent myotube formation in a circadian manner[47]. Similar differences may manifest in chondrocytes and explain the increased OA severity in *Cry2* versus *Cry1* deficient mice.

The present RNA-seq analysis of cartilage from *Cry2* KO mice shows that circadian rhythm is a dysregulated pathway and the most differentially expressed CR genes are *Nr1d1, Nr1d2, Dbp* and *Tef*, all known *Bmal1* targets[48] (and therefore putative *Cry2* direct targets in cartilage. In line with this observation, all 4 circadian factors *Nr1d1, Nr1d2, Dbp* and *Tef* are co-expressed between CT 8–12 in most peripheral tissues[49]. Interestingly, while *Nr1d1, Nr1d2* are transcriptional repressors sharing the same binding site (RORE element)[6]. *Dbp* and *Tef* on the other hand, are transcriptional activators that share the same binding site (D-box)[50]. The finding that 44 out of the 53 DEG are up-regulated, while only 9 (including *Cry2*) are down-regulated, is consistent with the function of *Cry2* as a transcriptional repressor.

The RNA-seq results also show that ECM is dysregulated and the most differentially expressed ECM genes are collagen (*Col*) *IV and XXII*. Since the loss of circadian genes results in Iower ECM expression in cartilage[51], this change in ECM was an expected outcome. The interesting finding is the identified type of collagen because there is no report that describes the relationship between CR and *Col IV* or *XXII*[35]. COL IV is distributed in articular cartilage damage and during different types of surgical cartilage repair, which suggests *ColIV* is relevant for the homeostasis of chondrocytes[52]. *COL22a1* is associated with the extrafibrillar matrix in cartilage[53] but its function is not well characterized. Angiogenesis was also identified as dyregulated pathway in the RNA-seq data and this is consistent with the histological findings of increased blood vessels in the subchondral bone of the *Cry2* KO mice with DMM-induced OA. *Cry2* KO mice also showed more severe synovial changes, and this may be in part related to the reported control by *Cry* of inflammatory gene expression in synoviocytes[51]. As observed in the PPI network, *Pdgfra* is a putative functional link between all three dysregulated pathways. Pdgfra is up-regulated in cartilage of *Cry2* KO mice and selective inhibitors have been developed[54] making it an interesting drug target for treatment of OA.

A limitation of the present study is that we used mice with global deletion of *Cry1* or *Cry2*. These mice manifest glucose intolerance and constitutively high levels of circulating corticosterone and this has been attributed to reduced suppression of the hypothalamic-pituitary-adrenal axis coupled with increased glucocorticoid transactivation in the liver[22]. It is thus possible that these metabolic abnormalities contribute to the increased OA severity in the DMM model, although these mice do not manifest developmental defects in joints or increased risk for spontaneous disease development[26,55,56]. Despite these potential confounders also affecting cartilage and other joint tissues, the present data from RNAseq analysis of cartilage suggest a direct role of *Cry* in chondrocytes and that *Cry* suppression as seen in human OA cartilage can contribute to OA.

In conclusion, *CRY2* is a circadian rhythm gene that is suppressed in OA cartilage. The present results provide support for the role of CR in regulating cartilage homeostasis and that approaches to maintain normal levels of *CRY* may be of therapeutic value in OA.

Supplementary Material

Refer to Web version on PubMed Central for supplementary material.

ACKNOWLEDGEMENTS

This study was supported by NIH grant AG049617.

The authors thank Gogce Crynen for assistance with the statistical analysis.

REFERENCES

1. Bush JR, Beier F. TGF-beta and osteoarthritis--the good and the bad. Nat Med 2013;19:667–9. [PubMed: 23744142]
2. Wu L, Huang X, Li L, Huang H, Xu R, Luyten W. Insights on biology and pathology of HIF-1alpha/−2alpha, TGFbeta/BMP, Wnt/beta-catenin, and NF-kappaB pathways in osteoarthritis. Curr Pharm Des 2012;18:3293–312. [PubMed: 22646092]
3. Akagi R, Akatsu Y, Fisch KM, Alvarez-Garcia O, Teramura T, Muramatsu Y, et al. Dysregulated circadian rhythm pathway in human osteoarthritis: NR1D1 and BMAL1 suppression alters TGF-beta signaling in chondrocytes. Osteoarthritis Cartilage 2017;25:943–51. [PubMed: 27884645]
4. Gachon F, Nagoshi E, Brown SA, Ripperger J, Schibler U. The mammalian circadian timing system: from gene expression to physiology. Chromosoma 2004;113:103–12. [PubMed: 15338234]
5. Dibner C, Schibler U, Albrecht U. The mammalian circadian timing system: organization and coordination of central and peripheral clocks. Annu Rev Physiol 2010;72:517–49. [PubMed: 20148687]
6. Cho H, Zhao X, Hatori M, Yu RT, Barish GD, Lam MT, et al. Regulation of circadian behaviour and metabolism by REV-ERB-alpha and REV-ERB-beta. Nature 2012;485:123–7. [PubMed: 22460952]
7. Takahashi JS, Hong HK, Ko CH, McDearmon EL. The genetics of mammalian circadian order and disorder: implications for physiology and disease. Nat Rev Genet 2008;9:764–75. [PubMed: 18802415]
8. Sato TK, Yamada RG, Ukai H, Baggs JE, Miraglia LJ, Kobayashi TJ, et al. Feedback repression is required for mammalian circadian clock function. Nat Genet 2006;38:312–9. [PubMed: 16474406]
9. Panda S, Antoch MP, Miller BH, Su AI, Schook AB, Straume M, et al. Coordinated transcription of key pathways in the mouse by the circadian clock. Cell 2002;109:307–20. [PubMed: 12015981]
10. Hughes CE, Little CB, Caterson B. Measurement of aggrecanase-generated interglobular domain catabolites in the medium and extracts of cartilage explants using Western blot analysis. Methods Mol Biol 2003;225:89–98. [PubMed: 12769477]
11. Yan J, Wang H, Liu Y, Shao C. Analysis of gene regulatory networks in the mammalian circadian rhythm. PLoS Comput Biol 2008;4:e1000193. [PubMed: 18846204]
12. Zhang R, Lahens NF, Ballance HI, Hughes ME, Hogenesch JB. A circadian gene expression atlas in mammals: implications for biology and medicine. Proc Natl Acad Sci U S A 2014;111:16219–24. [PubMed: 25349387]
13. Gossan N, Zeef L, Hensman J, Hughes A, Bateman JF, Rowley L, et al. The circadian clock in murine chondrocytes regulates genes controlling key aspects of cartilage homeostasis. Arthritis Rheum 2013;65:2334–45. [PubMed: 23896777]
14. Balsalobre A, Brown SA, Marcacci L, Tronche F, Kellendonk C, Reichardt HM, et al. Resetting of circadian time in peripheral tissues by glucocorticoid signaling. Science 2000;289:2344–7. [PubMed: 11009419]

15. Yoo SH, Yamazaki S, Lowrey PL, Shimomura K, Ko CH, Buhr ED, et al. PERIOD2::LUCIFERASE real-time reporting of circadian dynamics reveals persistent circadian oscillations in mouse peripheral tissues. Proc Natl Acad Sci U S A 2004;101:5339–46. [PubMed: 14963227]

16. Guo B, Yang N, Borysiewicz E, Dudek M, Williams JL, Li J, et al. Catabolic cytokines disrupt the circadian clock and the expression of clock-controlled genes in cartilage via an NFsmall ka, CyrillicB-dependent pathway. Osteoarthritis Cartilage 2015;23:1981–8. [PubMed: 26521744]

17. Dudek M, Gossan N, Yang N, Im HJ, Ruckshanthi JP, Yoshitane H, et al. The chondrocyte clock gene Bmal1 controls cartilage homeostasis and integrity. J Clin Invest 2016;126:365–76. [PubMed: 26657859]

18. Snelling SJ, Forster A, Mukherjee S, Price AJ, Poulsen RC. The chondrocyte-intrinsic circadian clock is disrupted in human osteoarthritis. Chronobiol Int 2016;33:574–9. [PubMed: 27019373]

19. Fisch KM, Gamini R, Alvarez-Garcia O, Akagi R, Saito M, Muramatsu Y, et al. Identification of transcription factors responsible for dysregulated networks in human osteoarthritis cartilage by global gene expression analysis. Osteoarthritis Cartilage 2018;26:1531–38. [PubMed: 30081074]

20. Cameron ML, Briggs KK, Steadman JR. Reproducibility and reliability of the outerbridge classification for grading chondral lesions of the knee arthroscopically. Am J Sports Med 2003;31:83–6. [PubMed: 12531763]

21. Pauli C, Whiteside R, Heras FL, Nesic D, Koziol J, Grogan SP, et al. Comparison of cartilage histopathology assessment systems on human knee joints at all stages of osteoarthritis development. Osteoarthritis Cartilage 2012;20:476–85. [PubMed: 22353747]

22. Lamia KA, Papp SJ, Yu RT, Barish GD, Uhlenhaut NH, Jonker JW, et al. Cryptochromes mediate rhythmic repression of the glucocorticoid receptor. Nature 2011;480:552–6. [PubMed: 22170608]

23. Carames B, Hasegawa A, Taniguchi N, Miyaki S, Blanco FJ, Lotz M. Autophagy activation by rapamycin reduces severity of experimental osteoarthritis. Ann Rheum Dis 2012;71:575–81. [PubMed: 22084394]

24. Rio DC, Ares M Jr., Hannon GJ, Nilsen TW. Purification of RNA using TRIzol (TRI reagent). Cold Spring Harb Protoc 2010;2010:pdb prot5439.

25. Alvarez-Garcia O, Olmer M, Akagi R, Akasaki Y, Fisch KM, Shen T, et al. Suppression of REDD1 in osteoarthritis cartilage, a novel mechanism for dysregulated mTOR signaling and defective autophagy. Osteoarthritis Cartilage 2016;24:1639–47. [PubMed: 27118398]

26. Thresher RJ, Vitaterna MH, Miyamoto Y, Kazantsev A, Hsu DS, Petit C, et al. Role of mouse cryptochrome blue-light photoreceptor in circadian photoresponses. Science 1998;282:1490–4. [PubMed: 9822380]

27. Glasson SS, Blanchet TJ, Morris EA. The surgical destabilization of the medial meniscus (DMM) model of osteoarthritis in the 129/SvEv mouse. Osteoarthritis Cartilage 2007;15:1061–9. [PubMed: 17470400]

28. Pritzker KP, Gay S, Jimenez SA, Ostergaard K, Pelletier JP, Revell PA, et al. Osteoarthritis cartilage histopathology: grading and staging. Osteoarthritis Cartilage 2006;14:13–29. [PubMed: 16242352]

29. Krenn V, Morawietz L, Haupl T, Neidel J, Petersen I, Konig A. Grading of chronic synovitis--a histopathological grading system for molecular and diagnostic pathology. Pathol Res Pract 2002;198:317–25. [PubMed: 12092767]

30. Matsuzaki T, Alvarez-Garcia O, Mokuda S, Nagira K, Olmer M, Gamini R, et al. FoxO transcription factors modulate autophagy and proteoglycan 4 in cartilage homeostasis and osteoarthritis. Science Translational Medicine 2018;10.

31. Dobin A, Davis CA, Schlesinger F, Drenkow J, Zaleski C, Jha S, et al. STAR: ultrafast universal RNA-seq aligner. Bioinformatics 2013;29:15–21. [PubMed: 23104886]

32. Liao Y, Smyth GK, Shi W. featureCounts: an efficient general purpose program for assigning sequence reads to genomic features. Bioinformatics 2014;30:923–30. [PubMed: 24227677]

33. Love MI, Huber W, Anders S. Moderated estimation of fold change and dispersion for RNA-seq data with DESeq2. Genome Biology 2014;15:550. [PubMed: 25516281]

34. Heinz S, Benner C, Spann N, Bertolino E, Lin YC, Laslo P, et al. Simple Combinations of Lineage-Determining Transcription Factors Prime cis-Regulatory Elements Required for Macrophage and B Cell Identities. Molecular Cell 2010;38:576–89. [PubMed: 20513432]
35. Szklarczyk D, Morris JH, Cook H, Kuhn M, Wyder S, Simonovic M, et al. The STRING database in 2017: quality-controlled protein-protein association networks, made broadly accessible. Nucleic Acids Research 2017;45:D362–D68. [PubMed: 27924014]
36. van der Horst GT, Muijtjens M, Kobayashi K, Takano R, Kanno S, Takao M, et al. Mammalian Cry1 and Cry2 are essential for maintenance of circadian rhythms. Nature 1999;398:627–30. [PubMed: 10217146]
37. Bunger MK, Walisser JA, Sullivan R, Manley PA, Moran SM, Kalscheur VL, et al. Progressive arthropathy in mice with a targeted disruption of the Mop3/Bmal-1 locus. Genesis 2005;41:122–32. [PubMed: 15739187]
38. Kc R, Li X, Voigt RM, Ellman MB, Summa KC, Vitaterna MH, et al. Environmental Disruption of Circadian Rhythm Predisposes Mice to Osteoarthritis-Like Changes in Knee Joint. J Cell Physiol 2015:2174–83. [PubMed: 25655021]
39. Gossan N, Boot-Handford R, Meng QJ. Ageing and osteoarthritis: a circadian rhythm connection. Biogerontology 2014:209–19. [PubMed: 25078075]
40. Honda KK, Kawamoto T, Ueda HR, Nakashima A, Ueshima T, Yamada RG, et al. Different circadian expression of major matrix-related genes in various types of cartilage: modulation by light-dark conditions. J Biochem 2013;154:373–81. [PubMed: 23940085]
41. Takarada T, Kodama A, Hotta S, Mieda M, Shimba S, Hinoi E, et al. Clock genes influence gene expression in growth plate and endochondral ossification in mice. J Biol Chem 2012;287:36081–95. [PubMed: 22936800]
42. Shearman LP, Sriram S, Weaver DR, Maywood ES, Chaves I, Zheng B, et al. Interacting molecular loops in the mammalian circadian clock. Science 2000;288:1013–9. [PubMed: 10807566]
43. Kriebs A, Jordan SD, Soto E, Henriksson E, Sandate CR, Vaughan ME, et al. Circadian repressors CRY1 and CRY2 broadly interact with nuclear receptors and modulate transcriptional activity. Proc Natl Acad Sci U S A 2017;114:8776–81. [PubMed: 28751364]
44. Anand SN, Maywood ES, Chesham JE, Joynson G, Banks GT, Hastings MH, et al. Distinct and separable roles for endogenous CRY1 and CRY2 within the circadian molecular clockwork of the suprachiasmatic nucleus, as revealed by the Fbxl3(Afh) mutation. J Neurosci 2013;33:7145–53. [PubMed: 23616524]
45. Koike N, Yoo SH, Huang HC, Kumar V, Lee C, Kim TK, et al. Transcriptional architecture and chromatin landscape of the core circadian clock in mammals. Science 2012;338:349–54. [PubMed: 22936566]
46. Huber AL, Papp SJ, Chan AB, Henriksson E, Jordan SD, Kriebs A, et al. CRY2 and FBXL3 Cooperatively Degrade c-MYC. Mol Cell 2016;64:774–89. [PubMed: 27840026]
47. Lowe M, Lage J, Paatela E, Munson D, Hostager R, Yuan C, et al. Cry2 Is Critical for Circadian Regulation of Myogenic Differentiation by Bclaf1-Mediated mRNA Stabilization of Cyclin D1 and Tmem176b. Cell Rep 2018;22:2118–32. [PubMed: 29466738]
48. Hatanaka F, Matsubara C, Myung J, Yoritaka T, Kamimura N, Tsutsumi S, et al. Genome-wide profiling of the core clock protein BMAL1 targets reveals a strict relationship with metabolism. Mol Cell Biol 2010;30:5636–48. [PubMed: 20937769]
49. Pizarro A, Hayer K, Lahens NF, Hogenesch JB. CircaDB: a database of mammalian circadian gene expression profiles. Nucleic Acids Res 2013;41:D1009–13. [PubMed: 23180795]
50. Falvey E, Marcacci L, Schibler U. DNA-binding specificity of PAR and C/EBP leucine zipper proteins: a single amino acid substitution in the C/EBP DNA-binding domain confers PAR-like specificity to C/EBP. Biol Chem 1996;377:797–809. [PubMed: 8997490]
51. Hand LE, Hopwood TW, Dickson SH, Walker AL, Loudon AS, Ray DW, et al. The circadian clock regulates inflammatory arthritis. FASEB J 2016;30:3759–70. [PubMed: 27488122]
52. Foldager CB, Toh WS, Christensen BB, Lind M, Gomoll AH, Spector M. Collagen Type IV and Laminin Expressions during Cartilage Repair and in Late Clinically Failed Repair Tissues from Human Subjects. Cartilage 2016;7:52–61. [PubMed: 26958317]

53. Koch M, Schulze J, Hansen U, Ashwodt T, Keene DR, Brunken WJ, et al. A novel marker of tissue junctions, collagen XXII. J Biol Chem 2004;279:22514–21. [PubMed: 15016833]

54. Lee JW, Hirota T, Kumar A, Kim NJ, Irle S, Kay SA. Development of Small-Molecule Cryptochrome Stabilizer Derivatives as Modulators of the Circadian Clock. ChemMedChem 2015;10:1489–97. [PubMed: 26174033]

55. Lamia KA, Sachdeva UM, DiTacchio L, Williams EC, Alvarez JG, Egan DF, et al. AMPK regulates the circadian clock by cryptochrome phosphorylation and degradation. Science 2009;326:437–40. [PubMed: 19833968]

56. Griebel G, Ravinet-Trillou C, Beeske S, Avenet P, Pichat P. Mice deficient in cryptochrome 1 (cry1 (−/−)) exhibit resistance to obesity induced by a high-fat diet. Front Endocrinol (Lausanne) 2014;5:49. [PubMed: 24782829]

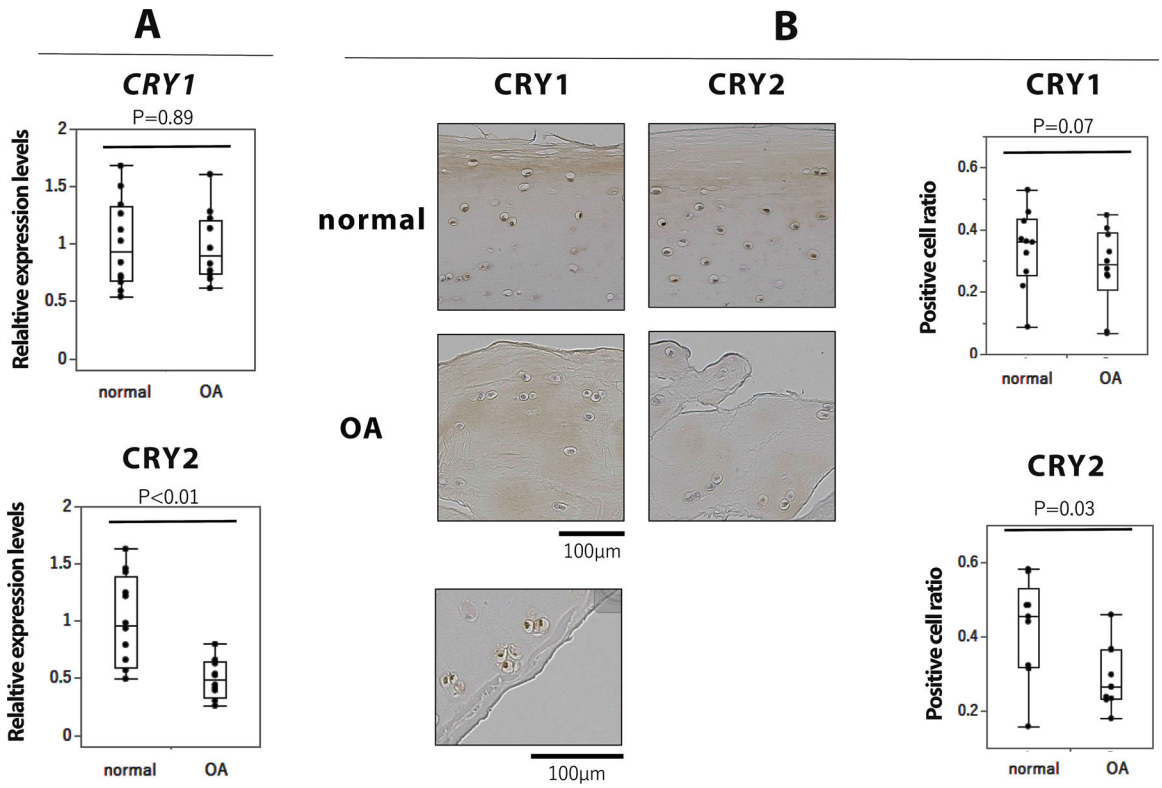

Figure 1. Expression of CRY1 and CRY2 mRNA and protein in normal and OA human cartilage.

(A) qPCR was performed on 12 normal and 12 OA human articular cartilage samples. For *CRY1*, the relative expression levels to *GAPDH* was 0.93 (0.68–1.32) in normal cartilage and 0.89 (0.74–1.2) in OA cartilage. For *CRY2*, the relative expression levels to *GAPDH* was 0.96 (0.59–1.38) in normal cartilage and 0.48 (0.33–0.64) in OA cartilage (Figure 1A). (B) Immunohistochemistry for CRY1 and CRY2. Protein expression was reduced in OA cartilage, although strong expression was observed in the cluster cells. For CRY1, the positive cell ratio was 0.36 (0.25–0.44) in normal cartilage and 0.29 (0.21–0.39) in OA cartilage. For CRY2, the positive cell ratio was 0.45 (0.32–0.53) in normal cartilage and 0.26 (0.23–0.37) in OA cartilage (n=10, each).

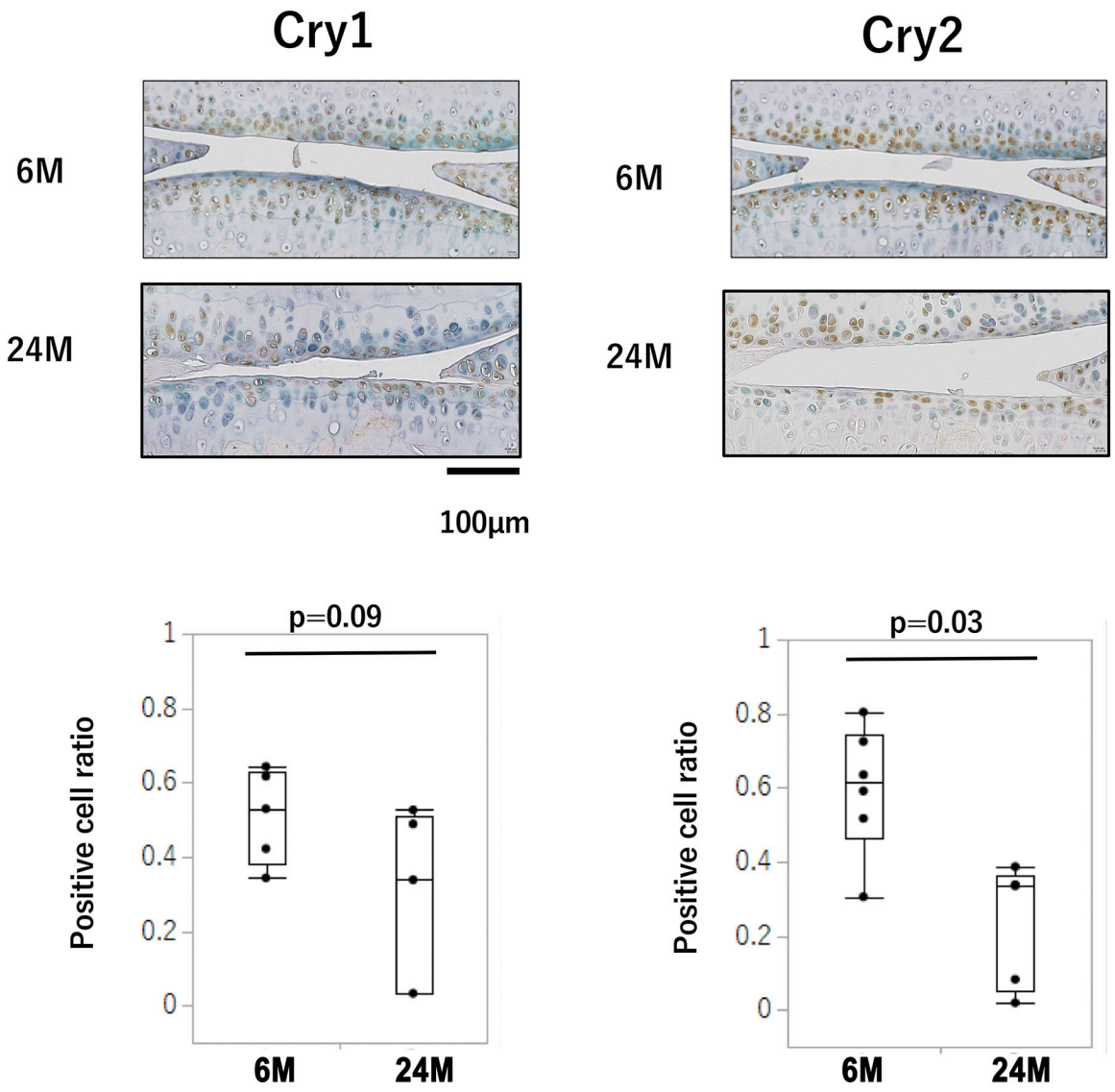

Figure 2. Cry expression in mouse joints.

Immunohistochemistry for Cry1 and Cry2. Representative images are shown for normal (6mo) and aged (24mo) cartilage. Sections were from the same 6mo or 24mo mice. Cry 1 and Cry2 positive cells were distributed mainly in the superficial to upper-mid zone. Expression levels were significantly reduced with aging at 24 months of age. mCry1 positive cell ratio was 0.53 (0.38–0.63) at 6 months and 0.33 (0.03–0.51) at 24 months cartilage. Cry2 positive cell ratio was 0.61 (0.46–0.74) at 6 months and 0.33 (0.05–0.36) at 24 months (n=5 or 6).

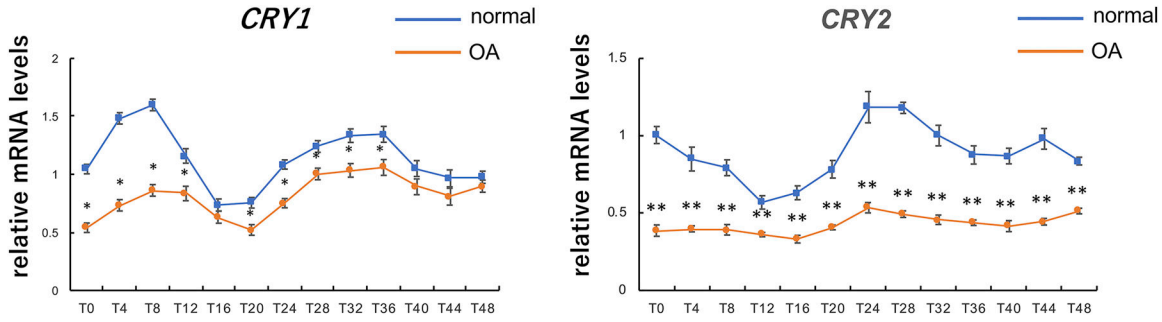

Figure 3. Circadian rhythmicity of *CRY* expression in normal and OA human chondrocytes.

RT-qPCR was performed on RNA isolated from 4 normal (blue lines) and 5 OA (red lines) human knee cartilage samples. Levels of *CRY1* mRNA expression peaked at Time (T)8 and T36, with lowest expression observed at T20. *CRY2* mRNA expression peaked at T24, with lowest expression at T12. In OA chondrocytes, *CRY2* expression was significantly reduced at all time points, *CRY* was reduced at some time points. *p<0.05; **p<0.01

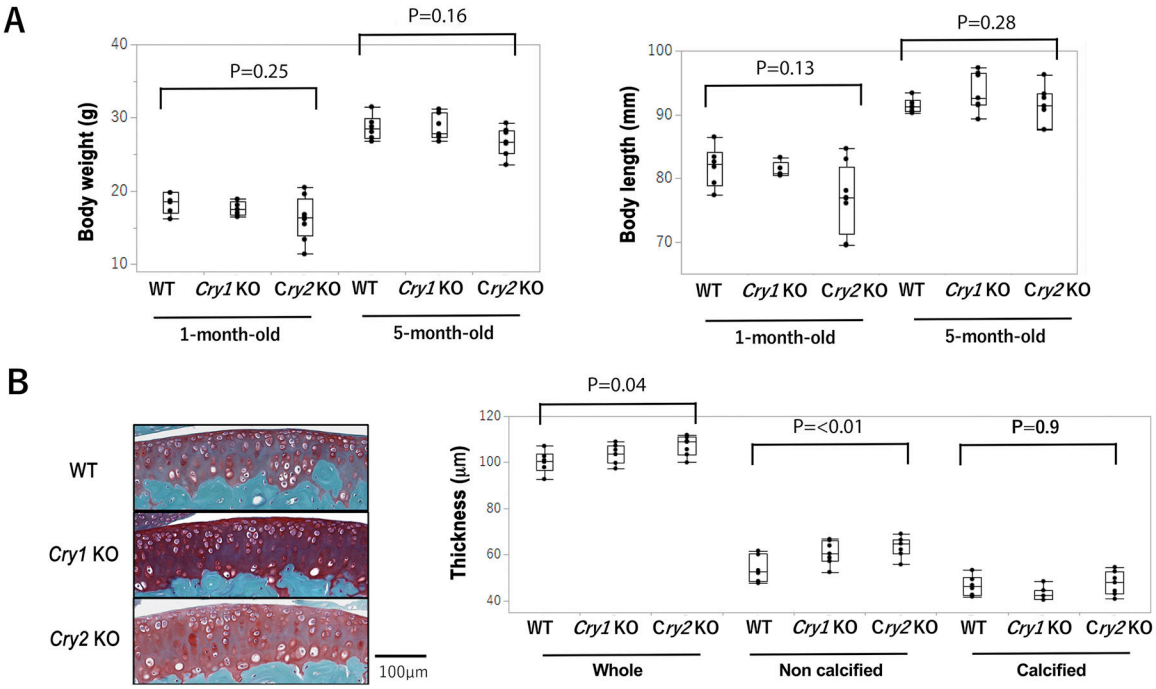

Figure 4. Skeletal and histological changes in *Cry* KO mice.

(A) Body weight and length of 1and 5 months-old WT or *Cry* KO mice.

(B,C) Histological sections of knee articular cartilage from 5 months-old mice.

The whole articular cartilage thickness was 100.6 (96.6–103.9) in WT, 103.6 (99.8–107.3) in *Cry1* KO and 108.9 (103.5–111) in *Cry2* KO mice. The height of non-calcified zone was 52.7 (48.4–60.6) in WT, 60.5 (57.3–66.3) in *Cry1* KO and 64.8 (60.6–66.5) in *Cry2* KO mice. The height of calcified zone was 46.2 (42.5–50.4) in WT, 42.3 (40.5–44.6) in *Cry1* KO and 48 (43.1–52.8) in *Cry2* KO mice (n=6 or 7).

KO: knock out, WT: wild type

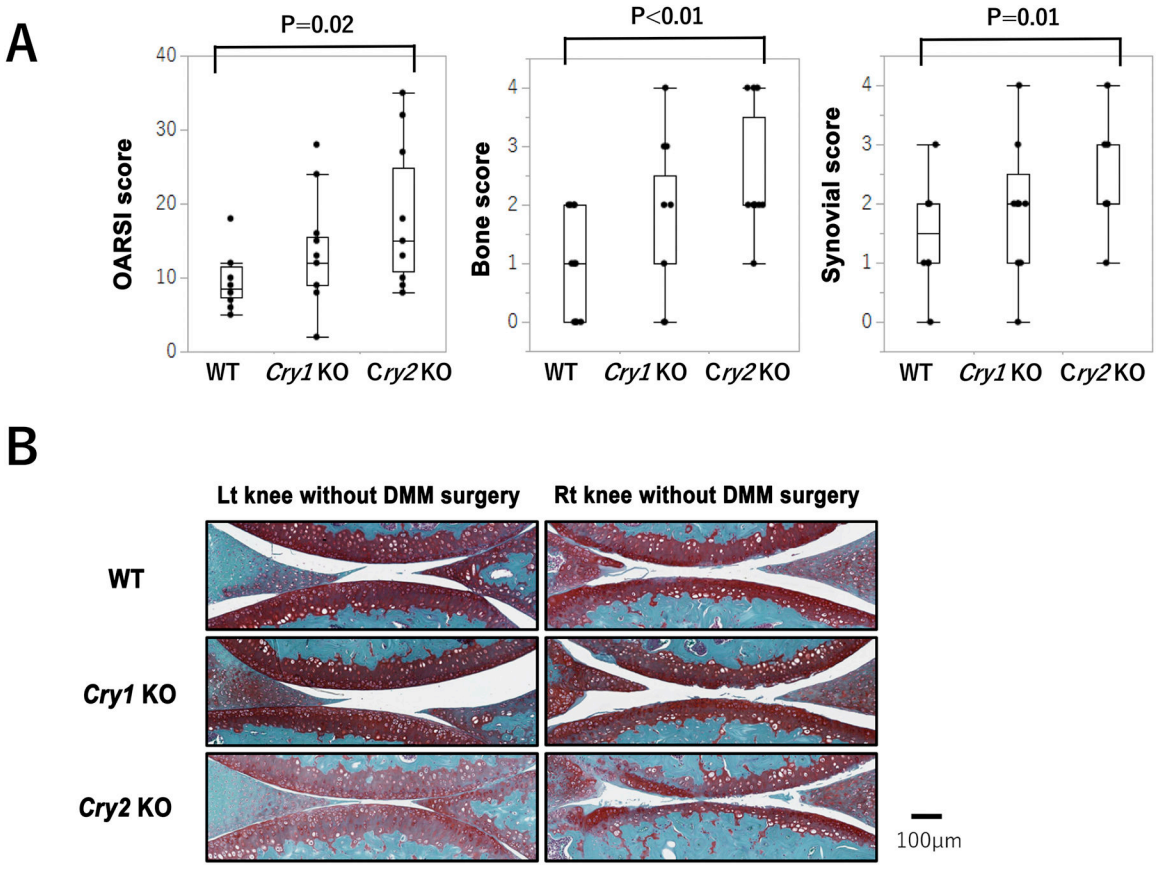

Figure 5. Increased severity of histopathological changes in knee joint tissues in *Cry* KO mice.

DMM surgery was performed in 3 months old mice and knee articular cartilage, synovium and subchondral bone were scored 8 weeks after DMM surgery. (A) OARSI scores. Bone and synovial scores. OARSI scores were 8.5 (7.3–11.5) in WT, 12 (0–15.5) in *Cry1* KO and 15 (10.8–24.8) in *Cry2* KO mice. Bone scores were 1 (0–2) in WT, 1 (1–2.5) in *Cry1* KO and 2 (2–3.5) in *Cry2* KO mice. Synovium scores were 1.5 (1–2) in WT, 2 (1–2.5) in *Cry1* KO and 3 (2–3) in *Cry2* KO mice. WT, 6 male, 6 female; *Cry1* KO, 7 male, 6 female; *Cry2* KO, 7 male, 5 female. (B) Representative knee sections, stained with Safranin O.

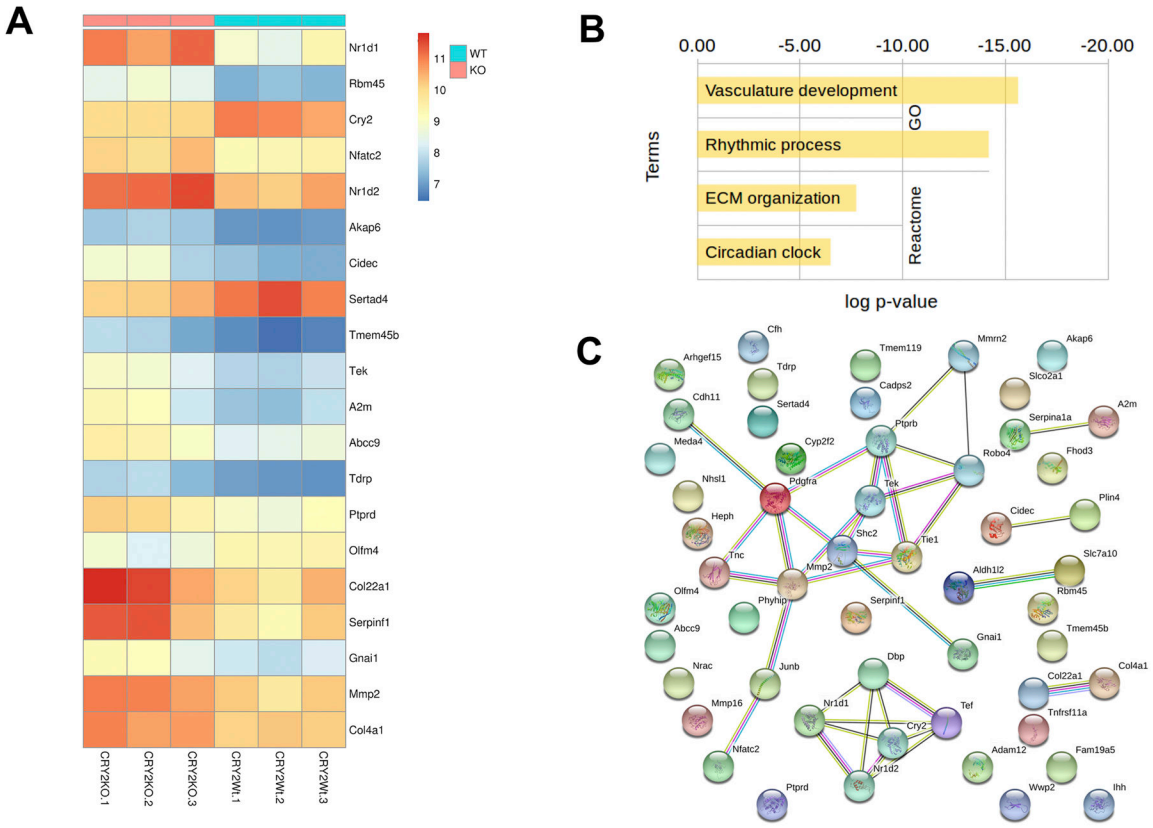

Figure 6. Differentially expressed genes in cartilage between WT and *Cry2* KO mice.

(A) Heatmap showing the variance stabilized transformed expression levels of the top 20 DEG. (B) Top 5 over-represented pathways among all 53 DEG in Reactome DB. (C) Protein-protein interaction network made with STRING DB of the DEG in cartilage of Cry2 KO mice. Interactions are color coded: Pink: experimentally determined, Light blue: from curated DBs, Green: gene neighborhood, Red: gene fusions, Blue: gene co-occurrence, Yellow: text mining, Black: co-expression, Purple: protein homology (n=3, each).